Available online at www.sciencedirect.com
ScienceDirect
Journal of the European Ceramic Society 28 (2008) 1213–1219
www.elsevier.com/locate/jeurceramsoc

Role of yttrium and magnesium in the formation of core-shell structure of $BaTiO_3$ grains in MLCC

Chang-Hoon Kim [a,*], Kum-Jin Park [a], Yeo-Joo Yoon [b], Min-Hee Hong [a], Jeong-Oh Hong [a], Kang-Heon Hur [c]

[a] *Material Development Group, LCR Division, Samsung Electro-Mechanics, Suwon, South Korea*
[b] *Analytical Research Group, Central R&D Institute, Samsung Electro-Mechanics, Suwon, South Korea*
[c] *LCR Development Team, LCR Division, Samsung Electro-Mechanics, Suwon, South Korea*

Received 20 June 2007; received in revised form 31 August 2007; accepted 8 September 2007
Available online 19 November 2007

Abstract

To understand the contribution of additive elements to the formation of core-shell structure in $BaTiO_3$ (BT) grains in multilayer ceramic capacitors, specimens were prepared with BT powders mixed with Y and Mg, and their microstructures were investigated in terms of scanning electron microscopy, X-ray diffractometry, and transmission electron microscopy. The additives inhibited growth of the BT grains, particularly leading to a much reduced sinterability for Y addition. Microstructural investigation showed that Y dissolved easily in BT lattice to a certain depth inside of the grain whereas Mg tended to stay at grain boundaries rather than to be incorporated into BT. It was considered that, added in a proper ratio, Y could play a dominant role in the formation of shell, leading to a slight dissolution of Mg in the shell.

Keywords: Sintering; Electron microscopy; $BaTiO_3$; Capacitors

1. Introduction

Development for Multilayer Ceramic Capacitor's (MLCC's) of a higher capacitance and a smaller chip size requires a structure in which hundreds of dielectric layers less than 1 μm thick are alternately stacked with inner electrodes. In such a thin layered structure, controlling the microstructure is difficult due to the effect of adjacent layers and the increased electric field intensity applied to the dielectric layer makes the reliability issue of great significance.[1,2] For 1 μm thick layers, $BaTiO_3$ (BT) grains need to be about 200 nm or less in size, and form a so-called 'core-shell' structure, in which the additive elements are partially dissolved in BT grains, to meet the requirements for the temperature dependence of the capacitance and the reliable performance in MLCC. The core-shell grain consists of the core region, pure BT with a ferroelectric tetragonal structure, surrounded by the shell which contains some additive elements and is pseudocubic.[3–6]

The most important in forming a core-shell structure is the selection of proper additives which leads to the reaction with dielectric grains. In BT–MgO–Ho_2O_3 system, Kishi et al. suggested a mechanism where Mg reacts with BT to form a shell at low temperatures and then, at a higher temperature, Ho reacts with the shell but its diffusion into the core is inhibited by Mg.[7] Chazono et al. reported that Nb and Co substituted for Ti-site in BT to form a shell in BT–Nb_2O_5–Co_3O_4 system.[8,9] In case of BT–MgO–Y_2O_3 system, Fujikawa et al. reported that Y dissolved in BT at 1200 °C followed by Ca incorporation into shell.[10] And, several different elements such as Zr, Yb, Sr, and Y have been reported as an element to form a shell.[11,12] In spite of the various studies, it is still unclear which element between rare earth and Mg plays a predominant role in forming a shell and what the formation mechanism of the shell is. Understanding the roles of different elements in the core-shell formation is critical to design a new material composition for a higher-level chip performance.

* Corresponding author.
E-mail address: ch1221.kim@samsung.com (C.-H. Kim).

0955-2219/$ – see front matter © 2007 Elsevier Ltd. All rights reserved.
doi:10.1016/j.jeurceramsoc.2007.09.042

In the present study, we selected Y and Mg as additives to study their contribution to the shell formation. BT ceramics were prepared with the addition of Y and Mg and their microstructures were investigated in terms of sinterability of BT grains and their core-shell structure formation.

2. Experimental procedure

It is known that at grain size below about 0.7 μm, the ferroelectricity of BT strongly decreases and its structure changes from tetragonal to pseudocubic.[13] In case of MLCC consisting of 200 nm dielectric grains, it is difficult to distinguish ferroelectric core from nonferroelectric shell in the grain. As a result, to facilitate the formation of core-shell structure in BT grain and its observation, specimens using BT powders of 400 nm nominal size with additives in $MgO–Y_2O_3–BaSiO_3$ system were prepared.

The starting powders were commercial-grade $BaTiO_3$ (Sakai Chemical), $MgCO_3$ (Kyorix), Y_2O_3 (Rhodia), $BaCO_3$ (Sakai Chemical) and SiO_2 (Kojundo Chemical). To study the contribution of Y and Mg in the shell formation, the relative amounts of them in total of 6 mol were varied as shown in Table 1.

The powders were weighed according to the nominal compositions, and mixed in water with dispersant by ball-milling for 12 h. The mixed powders were dried at 120 °C, granulated with polyvinyl alcohol, and pressed uniaxially into a disk of 15 mm diameter. The disks were baked at 400 °C for binder removal and annealed at 700 °C for 1 h to be mechanically robust during the following processes. The specimens were sintered at 1350 °C for 2 h in $H_2–H_2O–N_2$ atmosphere ($Po_2 \sim 10^{-9.3}$ Pa).

Bulk density of sintered specimen was measured using Archimedes method to check its sinterability, and the linear shrinkage behavior of the disk was investigated by dilatometry (Netzsch DIL402) in $H_2–N_2$ atmosphere and 10 °C/min heating rate. The disks were polished down to 0.3 μm grade, chemically etched, and then observed by scanning electron microscope (SEM, LEICA S440) to examine the grain size distribution.

The core-shell structure of BT grains was investigated in terms of X-ray diffractometry (XRD) and transmission electron microscopy (TEM). To check tetragonality (c/a) of the dielectric grains, XRD measurements (Rigaku, RINT 2200HF, Cu K_α) were carried out on powder or bulk specimens mainly in the range of 2θ value of 44–46.5°, covering (0 0 2) and (2 0 0) peaks of tetragonal BT, at 0.02° step.

TEM samples were prepared using tripod polishing followed by ion beam thinning (Gatan PIPS), and investigated using Tecnai G2 F20 microscope (FEI) operating at 200 kV. To investigate the elements in the shell region, energy dispersive spectrometry (EDS) line profiling over the grain were performed.

Table 1
Composition of ceramic specimens

Notation	$BaTiO_3$	$MgCO_3$	Y_2O_3	$BaCO_3$	SiO_2
6Y0Mg	100	0	3	2.5	2.5
4Y2Mg	100	2.0	2	2.5	2.5
3Y3Mg	100	3.0	1.5	2.5	2.5
2Y4Mg	100	4.0	1.0	2.5	2.5
0Y6Mg	100	6.0	0	2.5	2.5
R	100	0	0	2.5	2.5

Unit: mol.

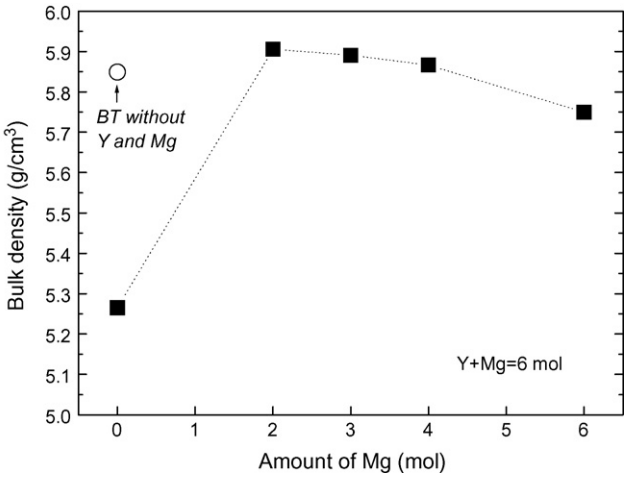

Fig. 1. Bulk density of the disk sintered at 1350 °C as a function of Mg amount.

3. Results and discussion

Fig. 1 shows the change of bulk density of the sintered disk according to the additive composition. The density of the specimen with proper amounts of Y and Mg was measured to be from 5.87 to 5.91 g/cm^3, comparable to that of the specimen without Y and Mg (5.85 g/cm^3). An increase of Mg amount induced a gradual decrease of the density while the specimen with Y only had the lowest density (5.26 g/cm^3) indicating that excessive addition of Y inhibited the densification of BT grains. These different sintering behaviors were confirmed by dilatometry measurements as shown in Fig. 2. Compared to 'R' specimen, the addition of Y and Mg retarded the onset of shrinkage to a higher temperature. And the specimen with more Y than Mg started to shrink later.

The cross sectional SEM images of the sintered disks are shown in Fig. 3. 'R' specimen consists of grains about 10 times

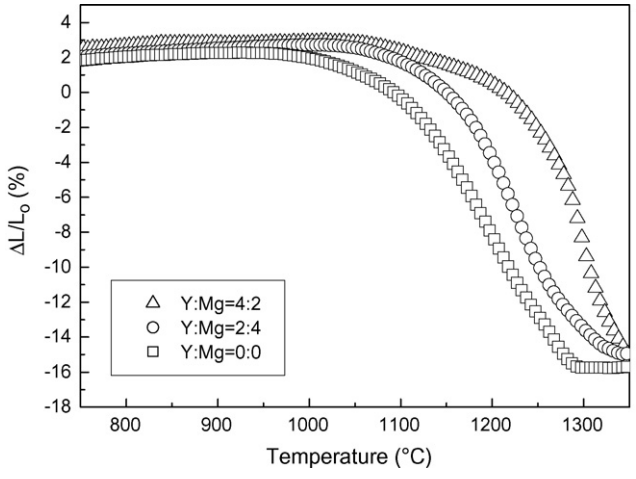

Fig. 2. Linear shrinkage of the disk in various compositions.

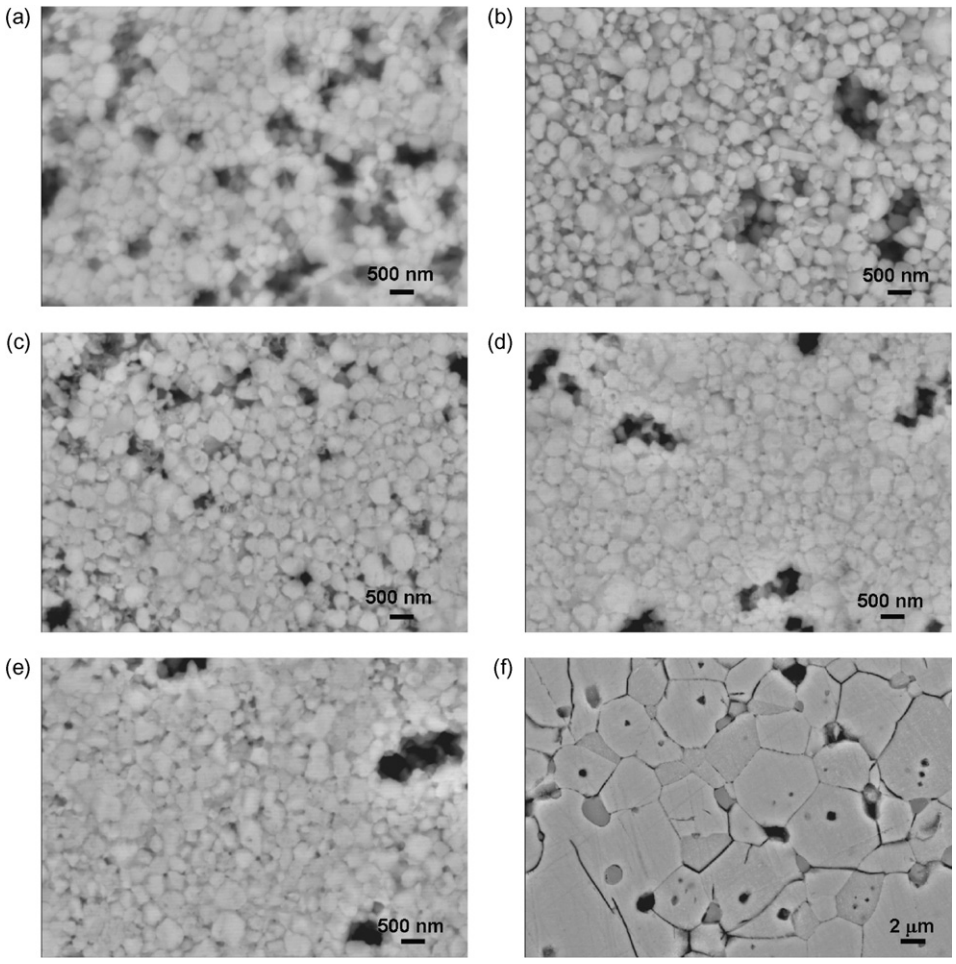

Fig. 3. Scanning electron micrographs of the cross sections of disks sintered at 1350 °C: (a) 6Y0Mg, (b) 4Y2Mg, (c) 3Y3Mg, (d) 2Y4Mg, (e) 0Y6Mg, (f) R specimen.

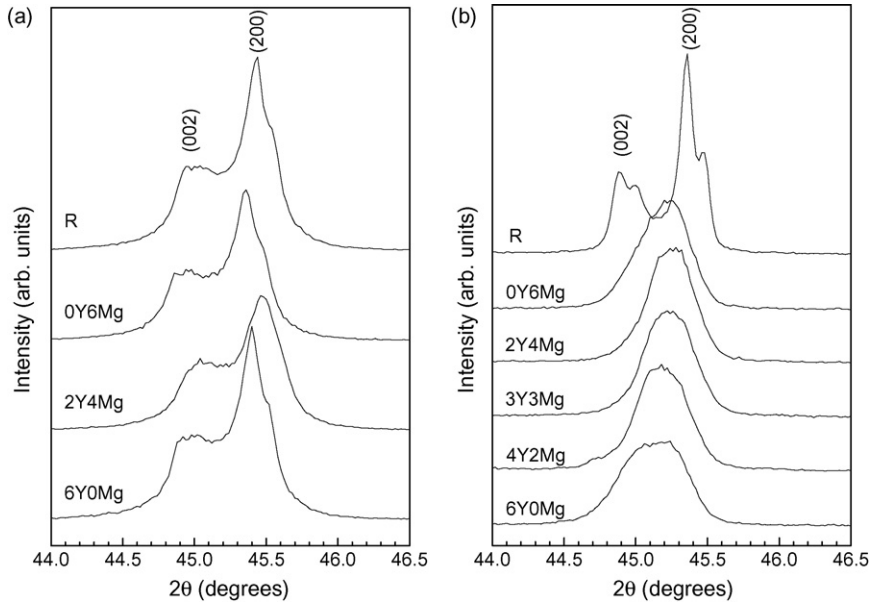

Fig. 4. XRD patterns of the specimens with various additive compositions: (a) powders dried after ball-milling, (b) disks sintered at 1350 °C.

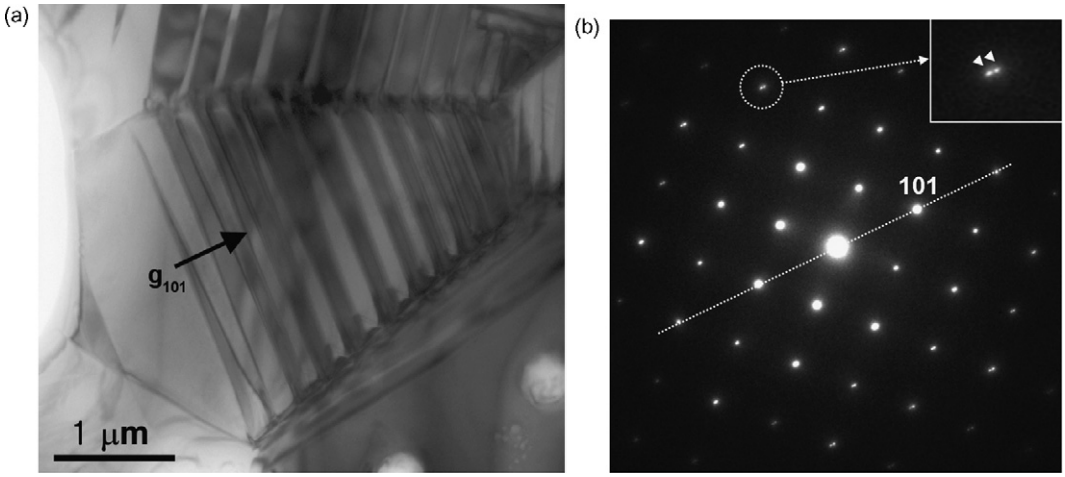

Fig. 5. (a) Transmission electron micrograph of a typical $BaTiO_3$ grain, showing ferroelectric domains, in 'R' specimen, (b) selected area electron diffraction pattern of the grain in (a) in (0 1 0) zone axis orientation; twin spots are magnified to show spot splitting.

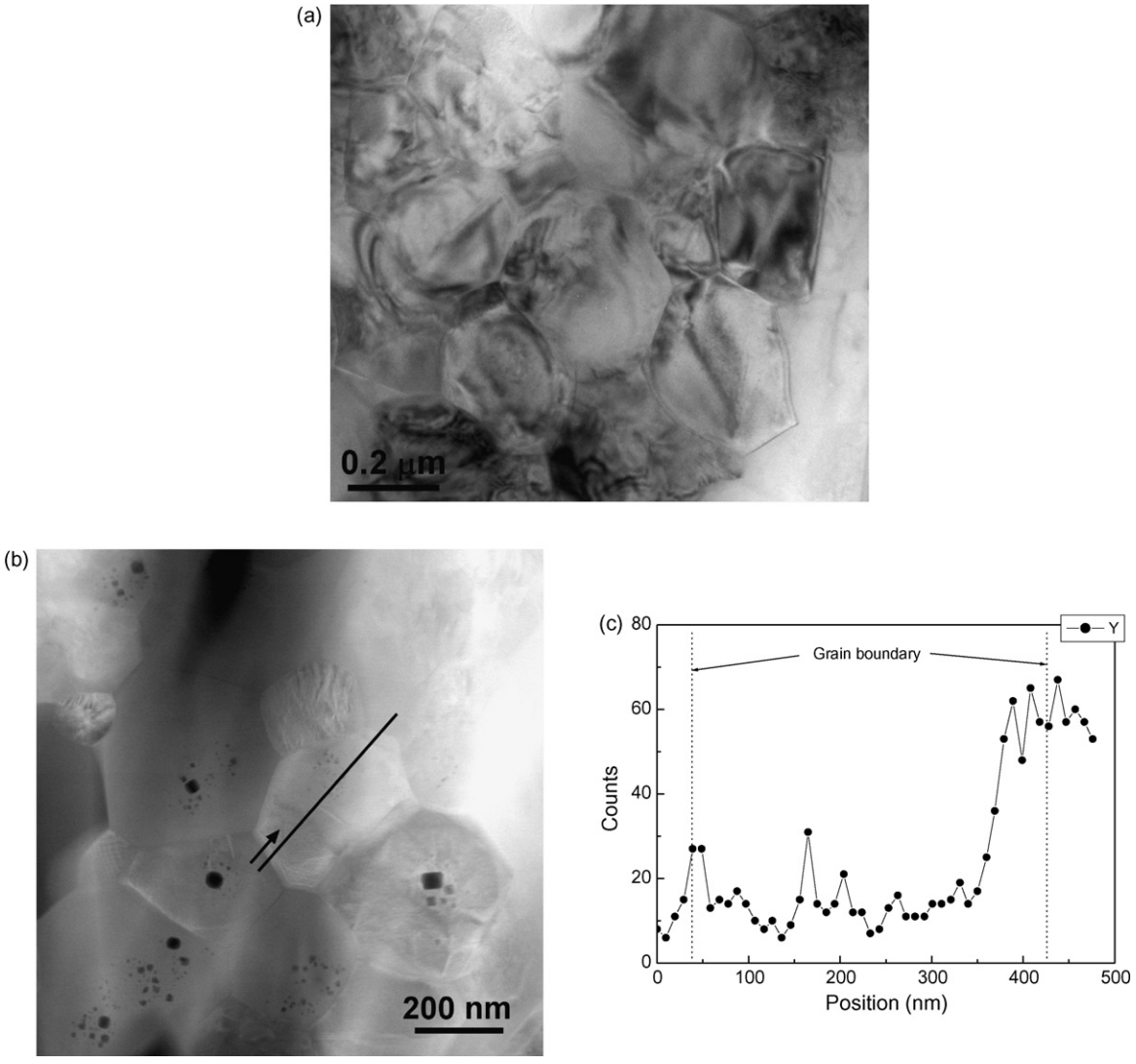

Fig. 6. (a) Transmission electron micrograph of typical dielectric grains in '6Y0Mg' specimen; no ferroelectric domains are visible. (b) and (c) EDS line profile on a grain showing the concentration gradient of Y within the grain.

larger than those of the specimens with additives; the median grain size was 4.74 (R), 0.365 (6Y0Mg), 0.352 (4Y2Mg), 0.355 (3Y3Mg), 0.349 (2Y4Mg), and 0.337 μm (0Y6Mg), respectively. The sintered specimens with additives showed similar grain sizes slightly less than the nominal raw powder size and almost no grain growth. The '6Y0Mg' specimen showed a relatively porous microstructure, which was attributed either to the low bulk density or to a selective etch-out of secondary phases during the chemical etching process. From these results, it seems that Y and Mg behave differently in the densification of BT grains, although leading to similar grain growth inhibition.

Fig. 4 shows the XRD patterns of the powders dried after ball-milling and the disks sintered at 1350 °C. The powders showed similar XRD patterns, irrespective of the additive composition, where the slight increase of intensity between (0 0 2) and (2 0 0) peaks is considered to result from particle size reduction during ball-milling (Fig. 4(a)). The sintered disks, however, showed a different behavior according to the additive composition. In 'R' specimen, the peaks reflected increased crystallinity (the appearance of $K_{\alpha 2}$ peak), tetragonality and K-factor (ratio of the intensity of (2 0 0) peak to that between (0 0 2) and (2 0 0) peaks) which mainly resulted from the growth of BT grains. The specimens with additives, however, showed one peak corresponding to a pseudocubic structure, although the peak in '6Y0Mg' specimen is somewhat broader than that in '0Y6Mg' specimen. It is known that the reaction of additives with BT enhances the intensity between (0 0 2) and (2 0 0) peaks.[8] This result implies the possibility of the reaction between additives and BT to some extent, which could be investigated using TEM.

A typical microstructure of the grains in 'R' specimen is shown in Fig. 5. There were well-developed 90° ferroelectric domain boundaries in the grain of about 4 μm size. The domain boundary is formed through cubic to tetragonal phase transition, and has an index of $\{1\,0\,1\}_{tet}$ plane. In Fig. 5(b), the electron diffraction pattern of the grain shows a splitting of diffraction spot resulting from the adjacent domains.

In '6Y0Mg' specimen, the TEM observation confirmed the porous microstructure again, and showed two interesting features; there were some features like strain contrast in the grain and most grains did not show 90° domains as shown in Fig. 6(a). In some cases, there were shell-like parts observed inside of the grain, and EDS line profiling across that region revealed that the Y concentration was preserved to a certain depth from the grain boundary and decreased toward the inside of the grain (Fig. 6(b) and (c)). Y has been reported to substitute for Ba-site at low doping concentrations, and as its concentration increases, it begins to dissolve in Ti-site, up to 12 at% at 1515 °C.[14] Consequently, in the case of the addition of Y, it is considered that Y dissolved easily in the BT grain to a certain depth, leading to the reduced tetragonality. However, it is not clearly understood why the BT grains with Y only did not show any domains. It could be possible that Y dissolved into core region to make the domains disappear, but the relatively abrupt decrease of Y concentration into the core region in Fig. 6(c) makes this hypothesis less feasible. More studies in detail are needed to resolve this issue.

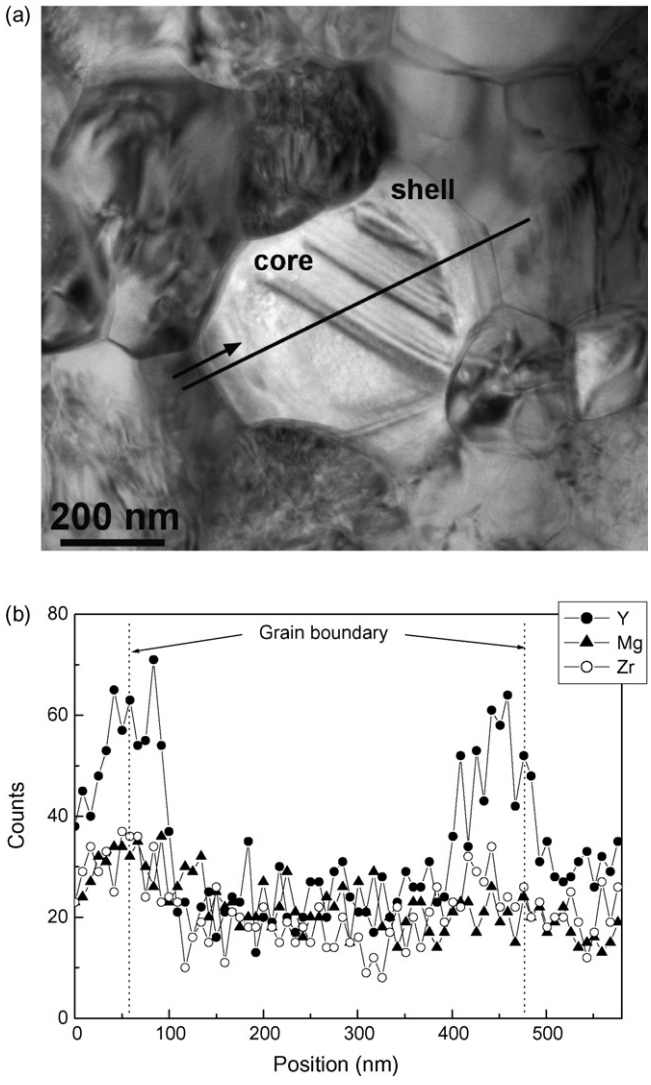

Fig. 7. (a) Transmission electron micrograph of a typical core-shell grain in '2Y4Mg' specimen, (b) EDS line profile on the grain in (a) indicating that Y is a dominant element in forming a shell.

The specimens added with proper ratios of Y to Mg (Y:Mg = 4:2, 3:3, 2:4) showed well-developed and easily-observed core-shell grains; a typical core-shell grain observed in '2Y4Mg' specimen is shown in Fig. 7(a). The core region is clearly distinguished from the shell in terms of the existence of domain boundaries. EDS line profile in Fig. 7(b) indicated that the concentration of Y decreased abruptly across the shell-to-core boundary and a little amount of Mg and Zr was also contained in the shell. Although the shell composition was slightly varied from grain to grain, it was generally confirmed that Y was a dominant additive element in forming a shell and Mg made a contribution to some extent. The Zr detected with Mg was attributed to contamination from ZrO_2 balls during the ball milling process.

In '0Y6Mg' specimen, which contained Mg only, the domain boundary in the grain was well observed, but the shell-like region

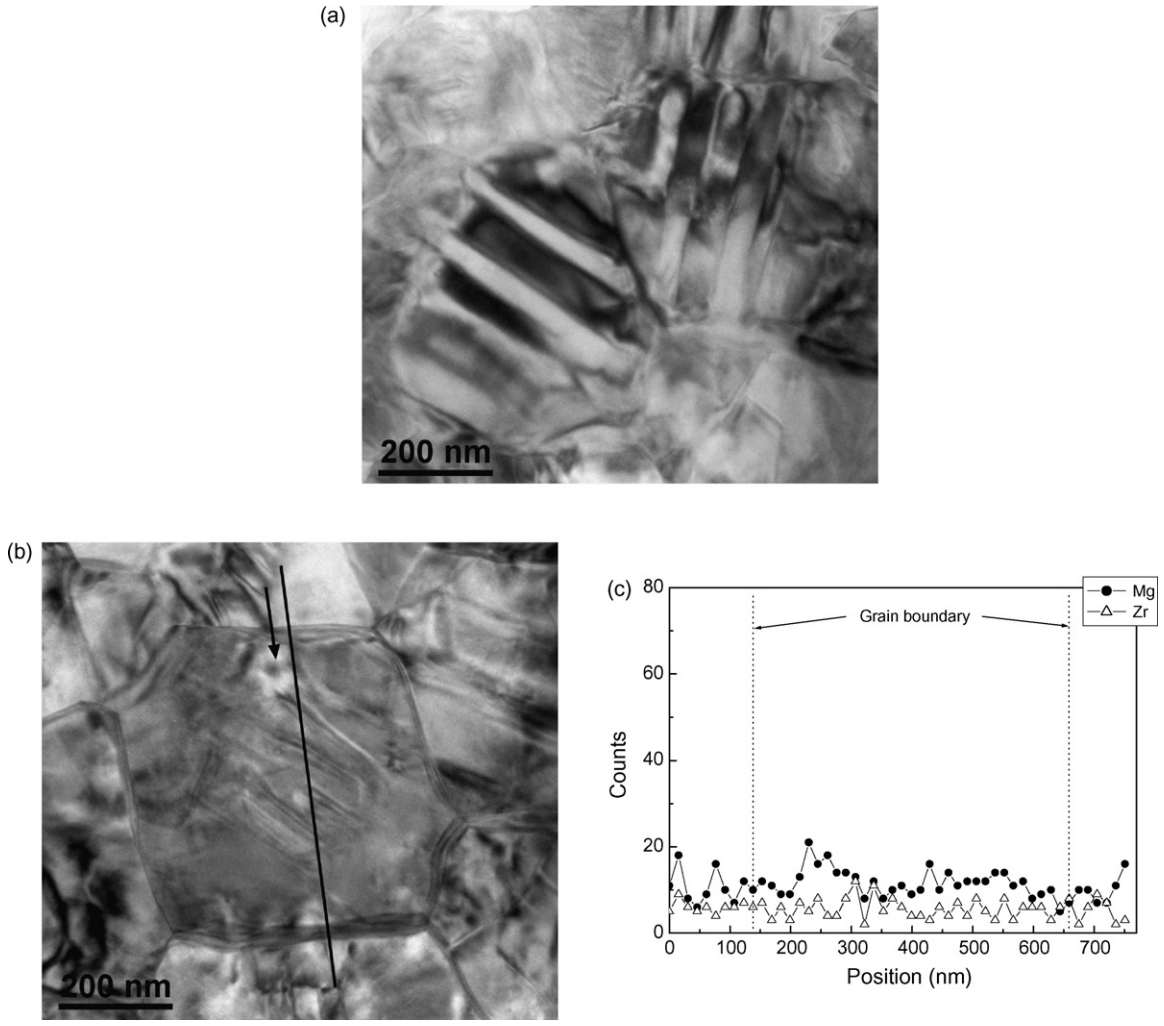

Fig. 8. (a) Transmission electron micrograph of a typical dielectric grain showing apparent domains in '0Y6Mg' specimen, (b) and (c) EDS line profile showing no concentration variation of Mg and Zr across one grain.

was hardly detected, as shown in Fig. 8(a). Moreover, EDS line profile did not show any concentration variation of Mg and Zr over the whole grain (Fig. 8(b) and (c)). Wada et al. reported that for BT powders synthesized hydrothermally and calcined at 800 °C, the maximum concentration of Mg dissolved in BT was about 0.15 wt%.[15] Therefore, the EDS result in Fig. 8(c) implies two possibilities; no dissolution of Mg in BT grain or the dissolution of a very small amount of Mg that was below the detection limit of our TEM EDS equipment. The XRD pattern of '0Y6Mg'specimen in Fig. 4(b), however, showed a pseudocubic peak as in other specimens of different additive compositions, which indicates that the additive would react with the dielectrics. To judge whether a shell has been formed, '0Y6Mg' specimen needs to be examined in a more detailed manner.

In addition to the difficulty in observing a shell, the TEM investigation of '0Y6Mg' specimen revealed another interesting fact; the existence of liquid phase at grain boundary. In Fig. 9, scanning transmission electron microscopy dark-field (STEM DF) image showed a dark contrast layer at the boundary between two adjacent dielectric grains, and EDS analysis detected relatively high intensities of Si and Mg at the same region. From these results, it is considered that Mg does not dissolve easily in the dielectric grain, compared to Y, but rather tends to stay in the liquid phase or even form a secondary phase.

It is obvious that in case of the addition of Mg only, Mg did not dissolve so easily into BT grain as Y. But, in the specimen with Mg and Y as shown in Fig. 7, Mg was slightly incorporated in the shell region within the grain, which implies that the lattice deformation resulting from the incorporation of Y into BT could make Mg dissolve more readily. According to the phase diagram study by Matraszek et al. in La_2O_3–Ga_2O_3–MgO–SrO system, it was experimentally observed that the solubility of Sr in $LaGaO_3$ phase at 1400 °C was less than 2 mol%. However, it increased up to about 20 mol% if Mg and Sr were added together.[16] As a result of the TEM analyses, it is considered that Y readily dissolves in BT lattice whereas Mg tends to stay at grain boundary instead of incorporation into BT. It is also considered that Y contributes mainly to forming a shell in the grain leading to an additional incorporation of Mg in the shell.

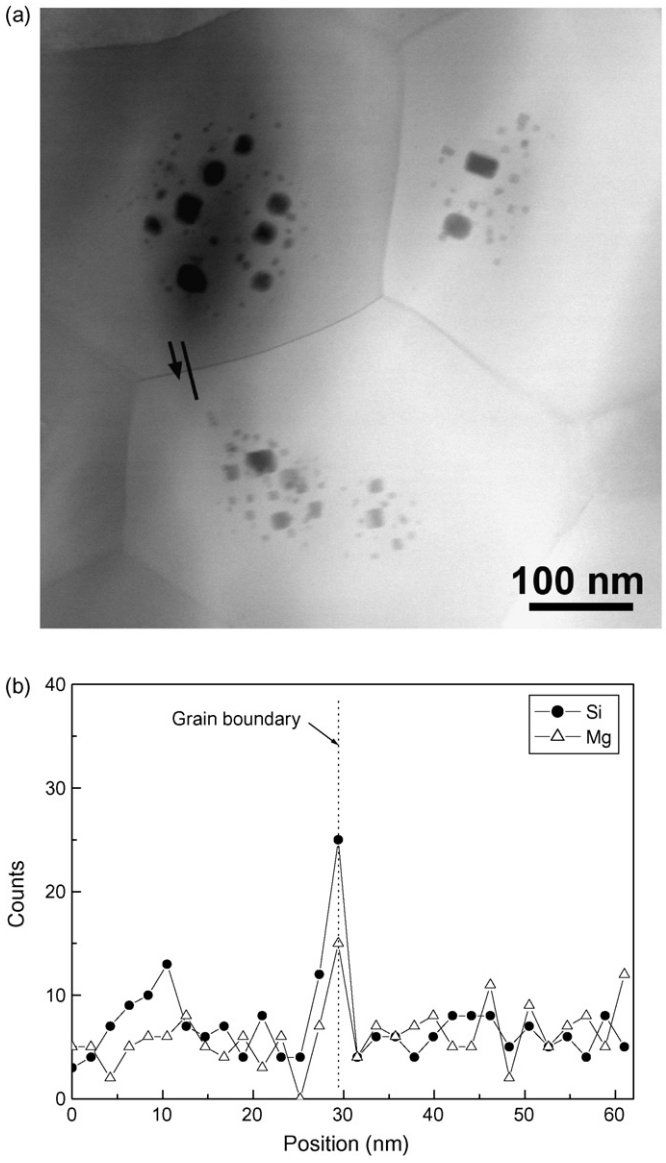

Fig. 9. (a) Scanning transmission electron micrograph and (b) EDS line profile for a grain boundary region in '0Y6Mg' specimen.

4. Conclusions

To investigate the contribution of additive elements to the formation of core-shell structure in $BaTiO_3$ grains, 400 nm BT powders were mixed with Y and Mg in various ratios to form ceramic disks and the microstructure of the sintered disks was investigated. Compared to BT without Y and Mg, the addition of additives inhibited growth of the dielectric grains, particularly showing a much reduced sinterability in case of Y addition. For the specimen added with Y only, Y dissolved easily in BT lattice to a certain depth inside of the grain whereas Mg tended to stay in the liquid phase instead of incorporation into BT. It is considered that in case of addition of Y and Mg in a proper ratio, Y could play a dominant role in the formation of shell, leading to a slight dissolution of Mg in the shell.

Acknowledgement

The authors are thankful to Prof. M. Martin of Aachen University of Technology for his helpful discussion.

References

1. Ohtani, O. and Takahara, W., Non-reducing dielectric ceramic composition. US 5403797, 1995.
2. Nomura, T., Nakano, Y., Satoh, A. and Arashi, T., Multilayer ceramic chip capacitor. US 5335139, 1994.
3. Hennings, D. and Rosenstein, G., Temperature-stable dielectrics based on chemically inhomogeneous $BaTiO_3$. *J. Am. Ceram. Soc.*, 1984, **67**, 249–254.
4. Randall, C. A., Wang, S. F., Laubscher, D., Dougherty, J. P. and Huebner, W., Structure property relationships in core-shell $BaTiO_3$-LiF ceramics. *J. Mater. Res.*, 1993, **8**, 871–879.
5. Yoon, S. H., Lee, J. H., Kim, D. Y. and Hwang, N. M., Core-shell structure of acceptor-rich, coarse barium titanate grains. *J. Am. Ceram. Soc.*, 2002, **85**, 3111–3113.
6. Armstrong, T. R. and Buchanan, R. C., Influence of core-shell grains on the internal stress state and permittivity response of zirconia-modified barium titanate. *J. Am. Ceram. Soc.*, 1990, **73**, 1268–1273.
7. Kishi, H., Okino, Y., Honda, M., Iguchi, Y., Imaeda, M., Takahashi, Y., Ohsato, H. and Okuda, T., The effect of MgO and rare-earth oxide on formation behavior of core-shell structure in $BaTiO_3$. *Jpn. J. Appl. Phys.*, 1997, **36**, 5954–5957.
8. Chazono, H. and Fujimoto, M., Sintering characteristics and formation mechanisms of core-shell structure in $BaTiO_3$-Nb_2O_5-Co_3O_5 ternary system. *Jpn. J. Appl. Phys.*, 1995, **34**, 5354–5359.
9. Chazono, H. and Kishi, H., Sintering characteristics in $BaTiO_3$-Nb_2O_5-Co_3O_4 ternary system. I. Electrical properties and microstructure. *J. Am. Ceram. Soc.*, 1999, **82**, 2689–2697.
10. Fujikawa, Y., Umeda, Y. and Yamane, F., Analysis on the sintering process of X7R MLCC materials. *J. Jpn. Soc. Powder Powder Metall.*, 2004, **51**, 839–844.
11. Grogger, W., Hofer, F., Warbichler, P., Feltz, A. and Ottlinger, M., Imaging of the core-shell structure of doped $BaTiO_3$ ceramics by energy filtering TEM. *Phys. Stat. Sol.*, 1998, **A166**, 315–325.
12. Chen, C. S., Chou, C. C. and Lin, I. N., Microstructure of X7R type base-metal-electroded BaTiO3 capacitor materials co-doped with MgO/Y_2O_3 additives. *J. Electroceram.*, 2004, **13**, 567–571.
13. Arlt, G., Hennings, D. and de With, G., Dielectric properties of fine-grained barium titanate ceramics. *J. Appl. Phys.*, 1985, **58**, 1619–1625.
14. Zhi, J., Chen, A., Zhi, Y., Vilarinho, P. M. and Baptista, J., Incorporation of yttrium in barium titanate ceramics. *J. Am. Ceram. Soc.*, 1999, **82**, 1345–1348.
15. Wada, S., Yano, M., Suzuki, T. and Noma, T., Crystal structure of barium titanate fine particles including Mg and analysis of their lattice vibration. *J. Mater. Sci.*, 2000, **35**, 3889–3902.
16. Matraszek, A., Singheiser, L., Kobertz, D., Hilpert, K., Miller, M., Schulz, O. and Martin, M., Phase diagram study in the La_2O_3-Ga_2O_3-MgO-SrO system in air. *Solid State Ionics*, 2004, **166**, 343–350.